

Activated Carbons as Electrode Materials in Electric Double-Layer Capacitors

I. Electrochemical Properties of Activated Carbons in Relation to their Porous Structures and Surface Oxygen Functional Groups

Chang-Hee Kim and Su-II Pyun[†]

Department of Materials Science and Engineering, Korea Advanced Institute of Science and Technology, Daejeon 305-701, Korea

(Received July 1, 2003; Accepted August 25, 2003)

ABSTRACT

This article is concerned with the overview of activated carbons as electrode materials in electric double-layer capacitors. Firstly, this article introduced various types of activated carbons with their precursors and manufacturing conditions which can be divided into two main steps of the carbonization and activation processes. Secondly, the present article gave the detailed discussion about the porous structures and examined previous works on the electrochemical behaviors of activated carbons in relation to their porous structures, along with our recent works. Finally, this article characterized the surface oxygen functional groups and presented their influence on the electrochemical properties of activated carbons by reviewing our recent results.

Key words : *Electric double-layer capacitors, Activated carbons, Electrode materials, Porous structures, Surface oxygen functional groups*

1. Introduction

Over the last two decades, the Electric Double-Layer Capacitors (EDLCs) have been receiving increased attention as pulsed power applications in energy storage systems.¹⁻³⁾ In the EDLCs, the energy storage is achieved electrostatically by the separation of electronic and ionic charges at the interface between electrode and electrolyte.⁴⁻⁶⁾ Owing to their non-faradaic character in the charge storage process, the EDLCs have special advantages in rate capability and cycle life as compared with the modern secondary batteries.

In general, highly porous activated carbons are used as the electrode materials in EDLCs, due to such advantageous features as high surface area and good electrical conductivity. Unfortunately, however, these advantages have proven not to be enough to realize the high power application of EDLCs, because the pores of the carbon electrodes are electrochemically accessible only through a cumulative solution resistance inside the pores. Moreover, it was reported⁷⁾ that the surface oxygen functional groups formed on the carbon electrodes affect the EDLC performance. Therefore, a great interest has been focused on the characterization of both the porous structures and the surface oxy-

gen functional groups, and their influence on the electrochemical properties of the activated carbons.^{8,9)}

The objective of this article is to overview the activated carbons as the electrode materials in EDLCs. For this purpose, we firstly introduced various types of activated carbons and manufacturing conditions inclusive of the carbonization and activation processes. Secondly, we gave the detailed discussion about the porous structures and correlated the porous structures with electrochemical behaviors of activated carbons. Finally, we characterized surface oxygen functional groups and their influence on the electrochemical properties of activated carbons.

2. Preparation of Activated Carbons

The term activated carbon in its broadest sense includes a wide range of amorphous carbon based materials prepared to exhibit a high degree of porosity and an extended surface area. These are obtained by carbonization of precursors, *i.e.*, raw materials with subsequent activation by physical treatment and/or chemical treatment. There are two general types of activated carbons, *i.e.*, powders (particle size lower than 0.18 mm) and granules (including extruded and pelletized), but there are other new forms such as fibers, cloths, and felts, which are recently attracting more and more attention.^{10,11)} Among them, powders and fibers are becoming increasingly useful in the application as electrode materials in electric double-layer capacitors, because they provide high surface area and good electrical properties.

The types of precursors and the varied manufacturing

[†]Corresponding author : Su-II Pyun

E-mail : sipyun@webmail.kaist.ac.kr

Tel : +82-42-869-3319 Fax : +82-42-869-3310

conditions used to produce carbonaceous materials are extensive.¹²⁾ Major precursors for activated carbon powders and granules are renewable fuels such as wood, nut shell, lignin, peat, etc. The common precursors for activated carbon fibers are pitches and polymeric materials such as rayon, phenolic resin, and Polyacrylonitrile (PAN). The porous structures of activated carbons are largely predetermined by the nature of precursors and the manufacturing conditions.

In general, the manufacturing conditions of the activated carbons involve two main steps: the carbonization of the precursors at temperature below 800°C in the absence of oxygen and the activation of the carbonized product.^{10,11)} During carbonization, most of the non-carbon elements such as oxygen and hydrogen are eliminated as volatile gaseous products by the pyrolysis decomposition of the precursors. The residual carbon atoms group themselves into sheets of condensed aromatic ring systems with a certain degree of planar structure. The mutual arrangement of these aromatic sheets is irregular and therefore leaves free interstices between them. These interstices give rise to pores, which make active carbons high surface area electrode materials.

The activation procedure is conducted in order to enhance the volume and to enlarge the diameter of pores that were already created during the carbonization process and to create some new porosity. Most commonly employed activation methods are divided into physical and chemical activations. In physical activation, the carbonized product is reacted at high temperature usually above 800°C with steam, carbon dioxide, or a mixture of these. Both carbon dioxide and steam are mild oxidant between 800° and 950°C, and eliminate carbon atoms from carbonized product via CO and/or CO+H₂, in such a way as to favor the selective burning of the interior of the particle, with the subsequent creation of porosity.¹⁰⁾

In chemical activation, the carbonized product is impregnated with a chemical agent, and the impregnated product is extruded and pyrolyzed between 400° and 600°C in the absence of air and then the pyrolyzed product is cooled and washed to remove the activating agent. The chemical agents used are normally KOH, NaOH, ZnCl₂, and H₃PO₄.¹³⁾ Since the temperature used in chemical activation is lower than that used in the physical activation process, the porous structure is more developed in the case of chemical activation.¹⁴⁻¹⁶⁾ The pore size of the activated carbons is determined by the degree of impregnation.

3. Porous Structures and their Correlations with Electrochemical Properties of Activated Carbons

3.1. Porous Structures of Activated Carbons

The structure of activated carbon is based on graphite lattice, although it exists in very defective form. It consists of graphite like layers of limited size stacked parallel to each

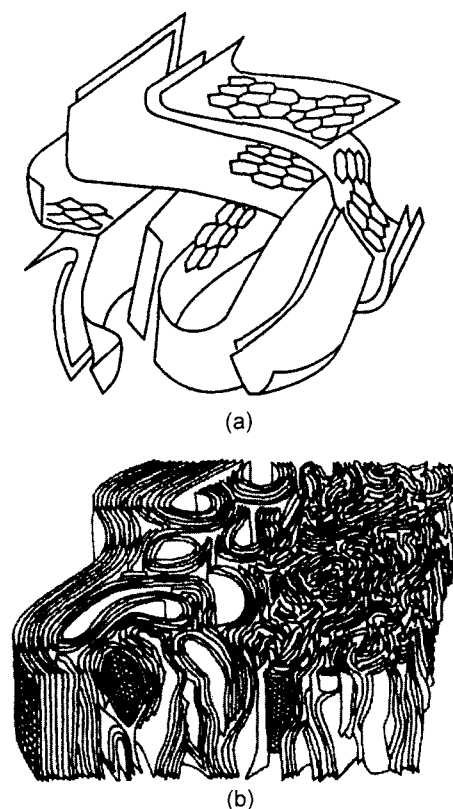


Fig. 1. Schematic representation of microstructures of (a) activated carbon powder¹⁸⁾ and (b) polyacrylonitrile-based activated carbon fiber.²⁰⁾

other without further ordering. The carbon-carbon distance within the layers is the same as in graphite. The d_{002} inter-layer spacing, however, is found to be larger than the value for single crystal graphite (typically ~0.344 nm).¹⁷⁾ Various forms of the activated carbons differ in size of the crystallites (from a few to a few tens nanometers) and in their mutual orientations.

The generally accepted microstructure of activated carbon powder is schematically represented in Fig. 1(a). It is a limiting case¹⁸⁾ of the model originally proposed by Oberlin *et al.*,¹⁹⁾ who investigated typical, but not activated, carbonaceous materials. The structure consists of aromatic sheets and strips, often bent and resembling a mixture of wood shavings and crumpled paper, with variable gaps of molecular dimensions between them. These variable gaps become the pores of the activated carbon powder. Of course, the highly disorganized structure of the material depends on the precursor and on its treatment. The micropores may be considered, locally at least, as slit shaped.¹⁸⁾

Several structure models of activated carbon fibers have been suggested in last two decades. Bennett *et al.*²⁰⁾ described the high strength and modulus PAN-based carbon fiber as shown in Fig. 1(b). They suggested that the structure is heterogeneous where some regions have good alignment of planes to the fiber axis, whereas others are crumpled and the resultant axial alignment is poor. The fibers are inter-

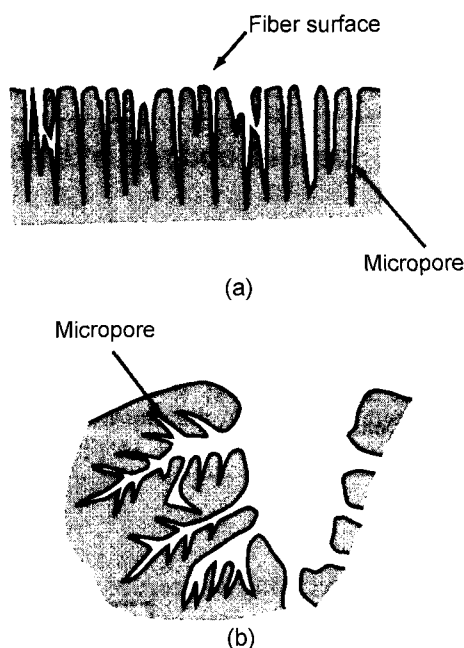


Fig. 2. Schematic representation of pore models of (a) activated carbon fiber and (b) activated carbon powder.²²⁾

spaced with pores oriented along the fiber axis. Recently, Daley *et al.*²¹⁾ reported that the porous structures of phenol-based activated carbon fibers are stable and homogeneous from the STM observation. The micropores are ellipsoidal in shape, and the pores are uniformly distributed throughout the bulk of the activated carbon fibers.

Fig. 2 presents comparative schematic pore structures of activated carbon fiber and activated carbon powder.²²⁾ The pores of activated carbon fiber open directly to the outer surface perpendicular to the fiber axis with minimum diffusion restriction, because of the narrow diameter of the fiber (10–20 μm). In contrast, for the carbon powder, the oxidation starts at the outer surface and gradually proceeds to the interior of the powder. Hence, the outer surface of the powder is more extensively oxidized to create the macropores of larger entrance diameters. Consequently, the outer zone and the core zone of the activated carbon powder have almost mesopores and micropores, respectively.

Following the International Union of Pure and Applied Chemistry (IUPAC) recommendations, the pores in activated carbons can be classified into three groups according to their size.²³⁾

(i) Pores with width (distance between the walls of a slit-shaped pore) not exceeding about 2 nm are called micropores

(ii) Pores of width between 2 nm and 50 nm are called mesopores

(iii) Pores with width exceeding about 50 nm are called macropores

Although most of the charge stored in the micropores of the activated carbons, meso- and macropores play a very important role in any charge accumulation, because they serve as a passage for the ions to the micropores.

3.2. Correlations of Porous Structures with Electrochemical Properties of Activated Carbons

The requirement of high surface areas of porous electrode structures is an obvious one for the development of high energy density of double-layer capacitor. However, it is not the only factor determining the performance characteristics of a double-layer capacitor based on high area porous electrodes. Several other factors enter into the optimization of electrode structures: two of the most important factors are the accessibility of electrolyte to the distributed pore area and the porous structure of the activated carbon.²⁴⁾

From the previous studies^{7,25)} on micropore accessibility to aqueous solution, it has been concluded that the size of a single nitrogen molecule is similar to that of hydrated ions, hence those micropores that can adsorb nitrogen molecules at 77 K are also available for the electrostatic-adsorption of simple hydrated ions under the pertaining experimental condition. In principle, the pores larger than about 0.4 nm could be accessible electrochemically for aqueous solutions. On the other hand in aprotic medium, taking into account the size of bigger solvated ions (e.g. the order of 2 nm for BF_4^- in propylene carbonate or 5 nm for $(\text{C}_2\text{H}_5)_4\text{N}^+$), the smaller non-accessible pores will not contribute to the total double-layer capacitance.²⁶⁾ Depending on the electrolyte medium, the convenient porous carbon materials should be selected for a capacitor electrode.

It is well known the porous structures of activated carbon electrodes are much more complicated: the pore shape is highly irregular, the pore size is nonuniformly distributed over the surface and the interior of the carbon electrodes as well, and the pores are branched and/or cross-linked.¹⁰⁾ Therefore, such analytical approaches as de Levies cylindrical pore model²⁷⁾ and fractal model^{28,29)} can not apply to the analysis of the electrochemical response of the porous carbon electrodes.

Miller³⁰⁾ first proposed the multi-RC-element ladder network as shown in Fig. 3, and numerically analyzed the electrochemical responses of the porous carbon electrodes with non-uniformly distributed pore size. Many researchers^{8,15)} have studied the kinetics of double-layer charging/discharging as a function of the Pore Size Distribution (PSD) of the porous carbon electrodes. However, in spite of its relevance, they disregarded the presence of the surface oxygen functional groups in investigating the effect of the PSD on the ion penetration into the pores during double-layer charging/discharging of the porous carbon electrode.

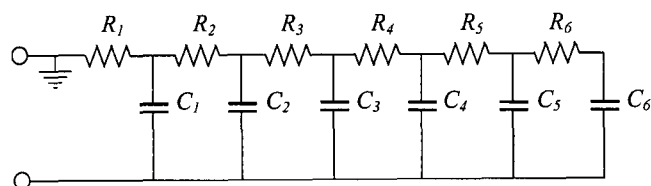


Fig. 3. Multi-RC-element ladder network used for the analysis of the resistive and capacitive responses of the carbon electrode.³⁰⁾

In view of the above circumstances, in our laboratory,^{31,32)} the kinetics of double-layer charging/discharging was investigated by preparing two types of As-Reactivated Carbon Powder Specimen (ARCPS) I and ARCPS II, which are characterized by almost the same concentration of the oxygen functional groups, but by different PSD. The average pore diameter of ARCPS I was determined to be 0.80 nm in value, which is smaller than that of ARCPS II 1.34 nm. On the other hand, the concentration of the oxygen functional groups of the ARCPS I was measured to be 0.34 mmol g⁻¹, which is almost the same in value as that of ARCPS II 0.32 mmol g⁻¹.

We determined six sets of RC elements for ARCPS I and ARCPS II by using the Complex Nonlinear Least-Squares (CNLS) fitting of the experimental impedance spectra to the six-RC-element ladder network. The time constant for each capacitive element was calculated from the product of the capacitance of that element and the series sum of all the resistive elements from that RC element to ground, because all the capacitive elements can be accessed only through a series connection of each resistive element.

Fig. 4 depicts the time constant distribution over the frequency f for the ARCPS I and ARCPS II. It is worthwhile to note that the ARCPS I always exhibited higher time constant than the ARCPS II at any given frequency during the penetration of the ions into the pores. This suggests that the carbon electrodes with smaller pores exhibit shorter ion penetration depth, and hence cause higher retardation in the ion penetration into the pores during double-layer charging/discharging of the carbon electrodes than the carbon electrodes with larger pores.

Fig. 5 plots of the reduced current density against the applied potential obtained from the ARCPS I and the ARCPS II at a scan rate v of 20 mV s⁻¹. The reduced current

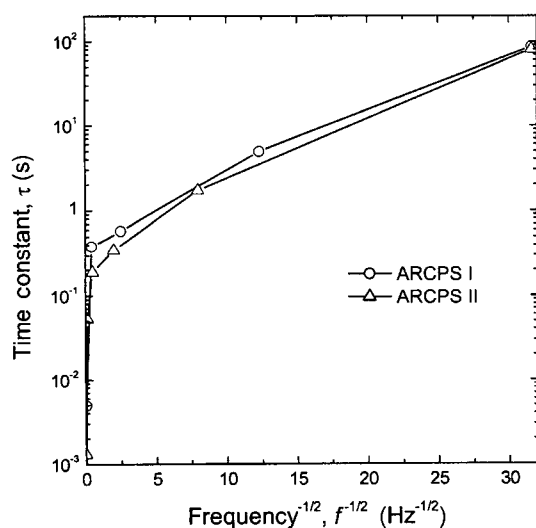


Fig. 4. Plots of the RC time constant τ against the inverse square root of frequency $f^{-1/2}$ for the ARCPS I (\circ) and the ARCPS II (\triangle), determined from the CNLS fitting of the experimental impedance spectra based on the six-RC-element ladder network in Fig. 3.

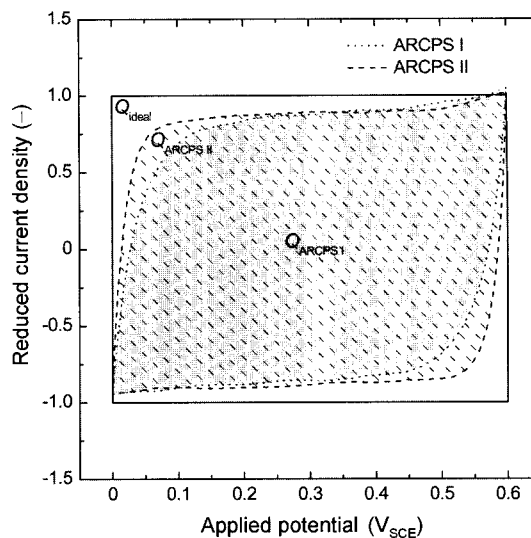


Fig. 5. Plots of the reduced current density against the applied potential obtained from the ARCPS I (dotted line) and the ARCPS II (dashed line). The reduced current density was calculated by dividing the current density by the steady-state current density $v C_{tot}/A_{BET}$ at a scan rate of 20 mV s⁻¹. Solid line represents the ideal double-layer capacitor where the time constant is zero.

density was calculated by dividing the current density by the steady-state current density $v C_{tot}/A_{BET}$. Here, C_{tot} represents the total capacitance and A_{BET} the BET surface area. The deviation from the ideal double-layer capacitor for the ARCPS I is more significant than that deviation for the ARCPS II, which is certainly ascribed to the higher time constant in the former carbon electrode specimen than that in the latter carbon electrode specimen.

Here, we quantitatively estimated the rate capability as the quotient of the reduced charge for the carbon electrode divided by the reduced charge for the ideal double-layer capacitor. The rate capability was determined to be 0.76 for the ARCPS I which is lower in value than that for the ARCPS II (0.83). From these results, it is concluded that the ion penetration into the carbon electrodes with smaller pores is more impeded than that into the carbon electrodes with larger pores during double-layer charging/discharging of the carbon electrodes.

4. Surface Oxygen Functional Groups and their Correlations with Electrochemical Properties of Activated Carbons

4.1. Surface Oxygen Functional Groups of Activated Carbons

The edge of the basal planes of carbon atoms in the graphite structure, where bonding in the plane is terminated, contains unsaturated carbon atoms. These sites are associated with high concentrations of unpaired electrons and, therefore, play a significant role in chemisorption. In crystalline graphite, the edge area is small as compared to that of the

basal plane, and graphite does not exhibit significant oxygen chemisorption. However, activated carbons have more disordered structures and more edge area, which result in a larger propensity for oxygen chemisorption. Moreover, since activated carbons are highly porous, they have high surface area, and hence high active surface area for chemisorption on the surface.

Two types of basic and acidic oxygen functional groups are generally known. Basic functional groups are formed always when a carbon surface is freed from all surface compounds by heating in a vacuum or in an inert atmosphere and comes into contact with oxygen only after cooling to low temperature.³³ As is known, the irreversible uptake of oxygen starts at ca. -40°C . Acidic functional groups are formed when the carbon is treated with oxygen at temperatures near its ignition point. It was found that the concentration of the oxygen functional groups increases with an increase in the oxidation temperature and reaches a maximum at 400° to 500°C .³⁴ At higher temperatures, the oxygen functional groups are thermally unstable and hence decompose to CO and CO_2 gases.¹¹ The oxygen functional groups are also formed on the reaction with oxidizing solution at room temperature.

The precise nature of surface oxygen functional groups is still not entirely established but the result of many studies^{11,35-37} using different experimental techniques concluded that there may be several types of oxygen functional groups, as shown in Fig. 6. The amounts and the types of oxygen functional groups of activated carbon depend very much on the manufacturing conditions, especially on the physical activation in carbon dioxide or steam.

Such oxygen functional groups influence the contact angle with the electrolyte under conditions of incomplete wetting of pores in capacitor-type, high surface area electrodes. The correlation between the contact angle of water and the carbon, and the quantity of oxygen associated with carbon blacks were investigated. As might be expected, electrochemical oxidation of carbons increases their wettability due to an increase in the oxygen content associated with hydrophilic surface groups.³⁸

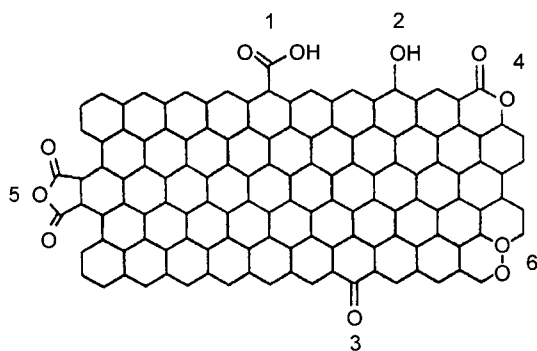


Fig. 6. Various types of surface oxygen functional groups formed on the carbon materials: 1. carboxyl; 2. phenolic; 3. quinon; 4. lactone; 5. carboxyl anhydride; 6. cycle peroxide groups.¹¹

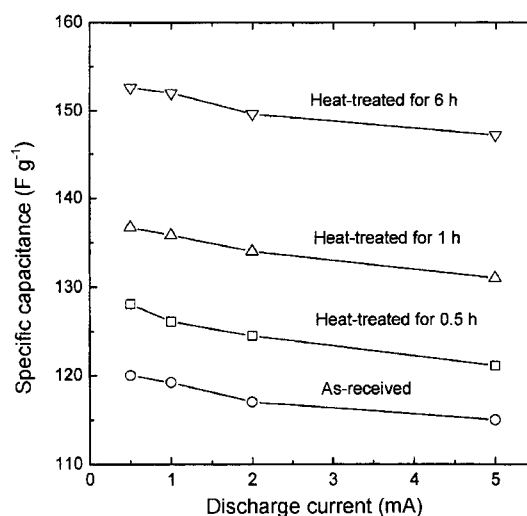


Fig. 7. Plots of specific capacitance vs. discharge current for the as-received activated carbon fiber electrode and the carbon fiber electrode heat-treated at 250°C under an oxygen atmosphere for 0.5, 1, and 6 h.³⁹ The activated carbon fiber electrodes were previously charged at 0.5 mA to 0.6 V (exposed area : 2 cm^2).

4.2. Correlations of Surface Oxygen Functional Groups with Electrochemical Properties of Activated Carbons

It was reported that the capacitance increased with the amount of surface oxygen functional groups on the carbon electrode. A previous study has also shown an increase of capacitance resulting from electrochemical oxidation of carbon electrode. Hsieh *et al.*³⁹ studied that influence of oxygen treatment on the capacitance of activated carbon fibers. In their work, 25% capacitance increase (e.g., from 120 to 150 F g^{-1} at a current density of 0.5 mA cm^{-2}) was achieved by thermal treatment of PAN-based activated carbon fiber at 250°C under an oxygen atmosphere for 6 h as shown in Fig. 7.

In an ideal formation of electric double-layer in the acidic electrolyte, the equilibrium reaction at the interface between the negative electrode and the electrolyte during charging is simply presented as



where $>\text{C}_x$ represents the carbon electrode surface, H^+ the proton of the acidic electrolyte, e an electron, and $>\text{C}_x // \text{H}^+$ the double-layer where the charges are accumulated on the two sides of the double-layer. The process is due to a simple physical adsorption, by electrostatic forces between the carbon surface and the proton. Basically, the numbers of ions involved in building the double-layer match the charge density developed on the electrodes.

The preceding analysis^{40,41} of oxygen functional groups formed on the activated carbon has shown that oxidized carbons contain a significant amount of carbonyl- or quinone-type groups, *i.e.*, $\text{C}=\text{O}$, on the surface. With the presence of these groups, an equilibrium reaction may occur in the car-

bon electrode by¹¹⁾



where $>C_xO//H^+$ represents a proton adsorbed by a carbonyl- or quinone-type site, basically induced by ion-dipole attraction. This specific adsorption process, which is different from the formation of $>C_x//H^+$ on non-specific sites through dispersion interactions,^{25,42)} may facilitate an excess specific double-layer capacitance due to the local changes of electronic charge density. It is thus suggested that the increase of capacitance upon oxidation arises partially from the enhanced dipole affinity towards protons in an acidic solution.

In charging the negative electrode, a strong bond may also form between quinone-type groups and protons due to electron transfer across the double-layer by



where $>C_xOH$ represents a hydroquinone-type complex. The reaction would proceed backwards during discharge. In pseudocapacitors, the charge is stored through the Faradaic reactions across the double-layer like in batteries, which gives rise to what is called pseudocapacitance.^{5,6)} Therefore, the oxygen functional groups, which would provide redox activity, may be responsible for faradaic current and thus the pseudocapacitance component of the overall capacitance of the oxidized carbon electrodes.²⁴⁾

The presence of surface oxygen functional groups on the carbon surface is not always beneficial because they serve to increase the leakage current.¹²⁾ The relationship between the apparent leakage current and the concentration of the surface oxygen functional groups of the activated carbon fiber electrode is demonstrated in Fig. 8.⁴³⁾ It is noteworthy that the apparent leakage current crucially depends on the

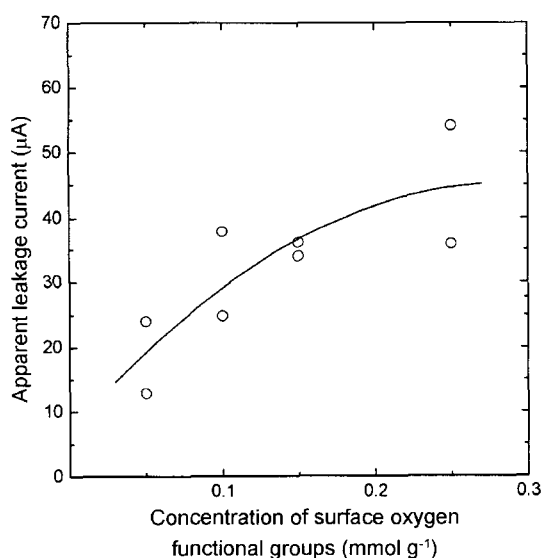


Fig. 8. Plot of the apparent leakage current vs. the concentration of the surface oxygen functional groups of the activated carbon fiber electrode.⁴³⁾

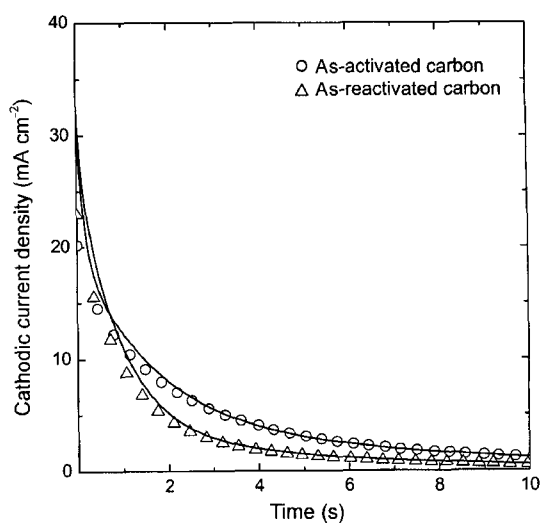


Fig. 9. The cathodic current transients experimentally obtained from the as-activated carbon (○) and as-reactivated carbon (△) electrode specimens in a 30 wt% H_2SO_4 solution by dropping the applied potential from 0.1 to 0.08 V_{SCE} (exposed area : 1 cm^2). Solid lines represent the simulated cathodic current transients.

concentration of the surface oxygen functional groups of the activated carbon fiber electrode.

In our recent work,^{31,32)} the role of surface oxygen functional groups in the kinetics of double-layer charging/discharging of activated carbon powder electrode specimens in a 30 wt% H_2SO_4 solution was investigated. In order to leave the effect of PSD out of consideration, we prepared two kinds of as-activated and as-reactivated carbon powder specimens, which are characterized by almost the same PSD, but by different concentration of the oxygen functional groups. The concentration of the oxygen functional groups of the as-activated carbon powder specimen was measured to be 1.35 $mmol\ g^{-1}$ which is much higher in value than that of the as-reactivated carbon powder specimen (0.34 $mmol\ g^{-1}$). However, the PSD of two types of the carbon specimens were exactly the same.

Fig. 9 envisages cathodic current transients (designated as open symbols) experimentally determined from the as-activated and as-reactivated carbon electrode specimens, together with those simulated (designated as solid lines). The simulation was performed from the circuit analysis using the SPICE based upon the six-RC-element ladder network in Fig. 3 at a potential step by taking the values of circuit elements obtained from the CNLS fitting method of experimental impedance spectra.

The experimental and simulated current transients coincided well with each other, indicating the time constant distribution of the carbon electrode crucially influences the current transients in value and shape. In particular, the current density for the as-activated carbon electrode specimen decayed more slowly with time as the ions penetrated into the pores than that current density for the as-reactivated carbon electrode specimen, which is due to higher

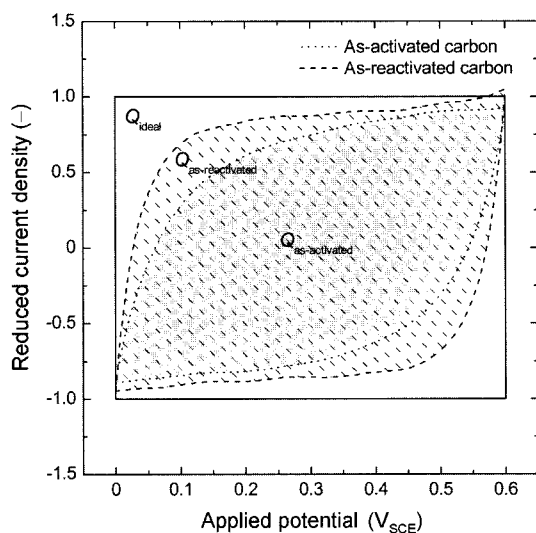


Fig. 10. Plots of the reduced current density against the applied potential obtained from the as-activated carbon (dotted line) and as-reactivated carbon (dashed line) electrode specimens. The reduced current density was calculated by dividing the current density by the steady-state current density $\nu C_{\text{tot}}/A_{\text{BET}}$ at a scan rate of 20 mV s^{-1} . Solid line represents the ideal double-layer capacitor where the time constant is zero.

time constant for the former carbon electrode specimen than that for the latter carbon electrode specimen.

It should be emphasized that the initial current level at $t=0$ for the as-activated carbon electrode specimen was smaller in value than that for the as-reactivated carbon electrode specimen. Since the same cell configuration was used throughout this work, the solution resistances were the same in both carbon electrode specimens. Therefore, it is reasonable to say that the resistance at or near the orifice of the pores of the as-activated carbon electrode specimen is larger as compared with that resistance at or near the orifice of the pores of the as-reactivated carbon electrode specimen. This is because the oxygen functional groups are mainly attached on the external surface where edge planes are predominant. Even though most of total surface area of activated carbon is composed of the internal surface area, the external surface area plays a very important role in charging/discharging rate, because it serves as a passage for the ions to the internal surface area.

From Fig. 10, the rate capability was determined to be 0.60 for the as-activated carbon electrode specimen. This value is lower than that for the as-reactivated carbon electrode specimen (0.76). From these results, we concluded that the surface oxygen functional groups impede the ion penetration into the pores during double-layer charging/discharging of the carbon electrodes.

Acknowledgement

This work was supported by a grant No. R01-2000-000-00240-0 from Korea Science & Engineering Foundation.

Incidentally, this work was partly supported by the Brain Korea 21 project.

REFERENCES

1. A. Soffer and M. Folman, "The Electrical Double Layer of High Surface Porous Carbon Electrode," *J. Electroanal. Chem.*, **38** 25-43 (1972).
2. A. Nishino, "Capacitors: Operating Principles, Current Market and Technical Trends," *J. Power Sources*, **60** [2] 137-47 (1996).
3. R. Kötz and M. Carlen, "Principles and Application of Electrochemical Capacitors," *Electrochim. Acta.*, **45** [15] 2483-98 (2000).
4. B. E. Conway, "Transition from Supercapacitor to Battery Behavior in Electrochemical Energy Storage," *J. Electrochem. Soc.*, **138** [6] 1539-48 (1991).
5. S.-I. Pyun, "Fundamentals of Battery and their Application into Practice," p. 403, Chungmungak, Seoul, 2003.
6. S.-I. Pyun, "Outlines of Electrochemistry at Materials," p. 561, Chungmungak, Seoul, 2003.
7. H. Shi, "Activated Carbons and Double Layer Capacitance," *Electrochim. Acta.*, **41** [10] 1633-39 (1996).
8. G. Salitra, A. Soffer, L. Eliad, Y. Cohen, and D. Aurbach, "Carbon Electrodes for Double-Layer Capacitors: I. Relations Between Ion and Pore Dimensions," *J. Electrochem. Soc.*, **147** [7] 2486-93 (2000).
9. D. Qu and H. Shi, "Studies of Activated Carbons Used in Double-Layer Capacitors," *J. Power Sources*, **74** [1] 99-107 (1998).
10. R. C. Bansal, J.-B. Donnet, and F. Stoeckli, "Active Carbon," pp. 1, 119, Marcel Dekker, Inc., New York and Basel, 1988.
11. K. Kinoshita, "Carbon: Electrochemical and Physicochemical Properties," p. 86, John Wiley & Sons, New York, 1988.
12. K. Kinoshita and X. Chu, "Carbon for Supercapacitors," pp. 171-80 in *Proceedings of the Symposium on Electrochemical Capacitors*, F. M. Denlick and M. Tomkiewicz, Eds., PV 95-29, The Electrochemical Society Proceeding Series, Pennington, NJ, 1995.
13. K. Gergova and S. Eser, "Effects of Activation Method on the Pore Structure of Activated Carbons from Apricot Stones," *Carbon*, **34** [7] 879-88 (1996).
14. T. Wigmans, "Industrial Aspects of Production and Use of Activated Carbons," *Carbon*, **27** [1] 13-22 (1989).
15. H. Teng and S.-C. Wang, "Preparation of Porous Carbons from Phenol Formaldehyde Resins with Chemical and Physical Activation," *Carbon*, **38** [6] 817-24 (2000).
16. T.-C. Weng and H. Ten, "Characterization of High Porosity Carbon Electrodes Derived from Mesophase Pitch for Electric Double-Layer Capacitors," *J. Electrochem. Soc.*, **148** [4] A368-73 (2001).
17. P. J. F. Harris, "Structure of Non-Graphitising Carbons," *Inter. Mater. Rev.*, **42** [5] 206-18 (1997).
18. H. F. Stoeckli, "Microporous Carbons and their Characterization: The Present State of the Art," *Carbon*, **28** [1] 1-6 (1990).
19. A. Oberlin, M. Villey, and A. Combaz, "Influence of Elemental Composition on Carbonization: Pyrolysis of Kero-

- sene Shale and Kuckersite," *Carbon*, **18** [5] 347-53 (1980).
20. S. C. Bennett and D. J. Johnson, "Electron-Microscope Studies of Structural Heterogeneity in PAN-Based Carbon Fibres," *Carbon*, **17** [1] 25-39 (1979).
 21. M. A. Daley, D. Tandon, J. Economy, and E. J. Hippo, "Elucidating the Porous Structure of Activated Carbon Fibers Using Direct and Indirect Methods," *Carbon*, **34** [10] 1191-200 (1996).
 22. H. Marsh and F. R. Reinoso, "Science of Carbon Materials," p. 287, Universidad de Alicante, Secretariado de Publicaciones, Spain, 2000.
 23. K. S. W. Sing, D. H. Everett, R. A. W. Haul, L. Moscou, R. A. Pierotti, J. Rouquerol, and T. Siemieniewska, "Reporting Physisorption Data for Gas/Solid Systems with Special Reference to the Determination of Surface Area and Porosity," *Pure & Appl. Chem.*, **57** 603-19 (1985).
 24. B. E. Conway, "Electrochemical Supercapacitors : Scientific Fundamentals and Technological Applications," p. 377, Kluwer Academic/Plenum Publishers, New York, 1999.
 25. J. Koresh and A. Soffer, "Double Layer Capacitance and Charging Rate of Ultramicroporous Carbon Electrodes," *J. Electrochem. Soc.*, **124** [9] 1379-85 (1977).
 26. E. Frackowiak and F. Beguin, "Review : Carbon Materials for the Electrochemical Storage of Energy in Capacitors," *Carbon*, **39** [6] 937-50 (2001).
 27. R. de Levie, "Advances in Electrochemistry and Electrochemical Engineering," p. 329, Ed., P. Delahay, Vol. **VI**, John Wiley, New York, 1967.
 28. B. B. Mandelbrot, D. E. Passoja, and A. J. Paullay, "Fractal Character of Fracture Surface of Metals," *Nature*, **308** 721-22 (1984).
 29. L. Nyikos and T. Pajkossy, "Fractal Dimension and Fractional Power Frequency-Dependent Impedance of Blocking Electrodes," *Electrochim. Acta.*, **30** [11] 1533-40 (1985).
 30. J. R. Miller, "Battery-Capacitor Power Source for Digital Communication Applications : Simulations Using Advanced Electrochemical Capacitors," pp. 246-54 in *Proceedings of the Symposium on Electrochemical Capacitors*, Eds., F. M. Denlick and M. Tomkiewicz, PV 95-29, The Electrochemical Society Proceeding Series, Pennington, NJ, 1995.
 31. C.-H. Kim, S.-I. Pyun, and H.-C. Shin, "Kinetics of Double-Layer Charging/Discharging of Activated Carbon Electrodes," *J. Electrochem. Soc.*, **149** [2] A93-8 (2002).
 32. S.-I. Pyun, C.-H. Kim, S.-W. Kim, and J.-H. Kim, "Effect of Pore Size Distribution of Activated Carbon Electrodes on Electric Double-Layer Capacitor Performance," *J. New Mater. Electrochem. Syst.*, **5** 289-95 (2002).
 33. B. S. Weller and T. F. Young, "Oxygen Complexes on Charcoal," *J. Am. Chem. Soc.*, **70** [12] 4155-62 (1948).
 34. H. W. Chang and S. K. Rhee, "Oxidation of Carbon Derived from Phenolic Resin," *Carbon*, **16** [1] 17-20 (1978).
 35. B. D. Epstein, E. Dalle-molle, and J. S. Mattson, "Electrochemical Investigations of Surface Functional Groups on Isotropic Pyrolytic Carbon," *Carbon*, **9** [5] 609-15 (1971).
 36. S. S. Barton, M. J. B. Evans, E. Halliop, and J. A. F. Mcdonald, "Acidic and Basic Sites on the Surface of Porous Carbon," *Carbon*, **35** [9] 1361-66 (1997).
 37. K. Shibagaki and S. Motojima, "Surface Properties of Carbon Micro-Coils Oxidized by a Low Concentration of Oxygen Gas," *Carbon*, **38** [15] 2087-93 (2000).
 38. K. Kinoshita and J. A. S. Bett, "Influence of Electrochemical Treatment in Phosphoric Acid on the Wettability of Carbons," *Carbon*, **13** [5] 405-09 (1975).
 39. C.-T. Hsieh and H. Teng, "Influence of Oxygen Treatment on Electric Double-Layer Capacitance of Activated Carbon Fabrics," *Carbon*, **40** [5] 667-74 (2002).
 40. S. Biniak, G. Szymanski, J. Siedlewski, and A. Swiatkowski, "The Characterization of Activated Carbons with Oxygen and Nitrogen Surface Groups," *Carbon*, **35** [12] 1799-810 (1977).
 41. C.-H. Kim, S.-I. Pyun, and J.-H. Kim, "An Investigation of the Capacitance Dispersion on the Fractal Carbon Electrode with Edge and Basal Orientations," *Electrochim. Acta.*, **48** [23] 3455-63 (2003).
 42. R. L. McCreery, K. K. Cline, C. A. McDermott, and M. T. McDermott, "Control of Reactivity at Carbon Electrode Surfaces," *Colloid Surface A*, **93** 211-19 (1994).
 43. A. Yoshida, I. Tanahashi, and A. Nishino, "Effect of Concentration of Surface Acidic Functional Groups on Electric Double-Layer Properties of Activated Carbon Fibers," *Carbon*, **28** [5] 611-15 (1990).